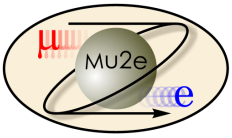

Tracking for next generation Mu2e

Eleonora Diociaiuti
Universita' degli Studi Roma Tre

Supervisor: Pasha Murat
Summer student 2015

September 25, 2015

ABSTRACT

In this report is described my Summer Student work in Fermilab. I worked in the Mu2e collaboration under the supervision of Dr P. Murat.
In Section 1 I briefly describe Mu2e experiment focusing on the experimental set up, the phisycal motivation and the the principal source of background.
In Section 2 I illustrate the tracker geometry in the current configuration and a new configuration proposal for Mu2e-2 underlining the possibility of improve Mu2e tracking at high rates.
In the last section I describe the segment reconstruction algorithm developed during this Summer Student Program and I show some preliminary results.

Fermilab

CONTENTS

1 MU2E EXPERIMENT

[1] [2]

Mu2e experiment purpuse is the measurment of the ratio of rate of the neutrinoless coherent conversion of muon into electrons in the field of a nucleos normalized to the rate of muon capture on nucleous

$$R_{\mu e} = \frac{\Gamma\left(\mu^- + A(Z,N) \rightarrow e^- + A(Z,N)\right)}{\Gamma\left(\mu^- + A(Z,N) \rightarrow \nu_\mu + A(Z-1,N)\right)} \tag{1}$$

The experimental signature is a mono-energetic electro with an energy similar to the muon rest mass.

1.1 Physics motivation

The conversion process is an example of Charged Lepton Flavor Violation process never observed experimentally. It's important to underline that the rate at which CLFV occurs is model-dependent, it result fundamental that experiments looking for CLFV event are sensitive to different processes in order to elucidate the mechanism responsible for flavor-violating effects. The most stringent limits currently come from the muon sector because of the high muon production rate and the long muon ife time. The studied rare muons decay modes are:

- $\mu^+ \rightarrow e^+\gamma$

- $\mu^+ \to e^+e^+e^-$
- $\mu^-N \to e^-N$

In Table 1 are listed upper limits of CLFV processes

$BR(\mu^+ \to e^+\gamma)$	$< 2.4x10^{-12}$
$BR(\mu^\pm \to e^\pm e^+e^-)$	$< 1.0x10^{-12}$
$BR(\mu^\pm \to \gamma\gamma)$	$< 7.2x10^{-11}$
$R\ (\mu^-Ti \to e^-Ti)$	$< 4.3x10^{-12}$
$R\ (\mu^-Au \to e^-Au)$	$< 710^{-13}$
$R\ (\mu^-Al \to e^-Al)$	-

Table 1: Data from current experimental limits at 90 % c.l.

The observation of this process would be a major discovery, signaling the existence of charged-lepton-flavor violation far beyond what is expected from current standard theory. A non-observation would be equally interesting as it would place stringent limits on theory and exclude large regions of parameter space for leading theories of beyond- standard-model physics

1.2 Experimental set up

The layout for the muon beam line and the detector system shows a typical S-shape : the entire system is surrounded by the Superconducting Solenoid Magnet System (Fig. 1)

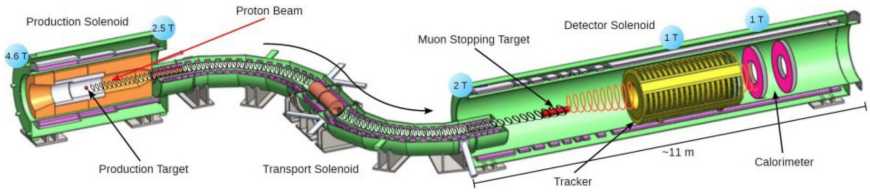

Figure 1: Schematic layout of the experimental apparatus

The solenoids can be divided into 3 units that will operate as a single:

- **Production Solenoid (PS)**: high field magnet with a graded solenoidal field from 4.6 Tesla to 2.5 Tesla. PS captures pions and muons coming from decays and guides them toward the Transport Solenoid.
- **Transport Solenoid (TS)**: set of superconducting solenoids and toroids that form a magnetic channel that transmits

low energy negatively charged muons from the Production Solenoid to the Detector Solenoid. Presence of absorbers and collimators along the TS stops negatively charged particles with high energy, positively charged particles and line-of-sight neutral particles.consists of five distinct regions: a 1 m long straight section, a 90° curved section, a second straight section about 2 m long, a second 90° curved section that brings the beam back to its original direction, and a third straight section of 1 m length.

- **Detector Solenoid (DS)**: large, low field magnet that houses the muon stopping target and the components required to identify and analyze conversion electrons from the stopping target. The muon stopping target resides in a graded field that varies from 2 Tesla to 1 Tesla. The graded field captures conversion electrons that are emitted in the direction opposite the detector components causing them to reflect back towards the detector.

The proton beam, with an energy of 8 GeV , coming from the Fermilab accelerator system, enters the Production Solenoid, and hit the production target. After a selection in charge reaction products are transported through the S-shaped Transport Solenoid, which is long enough to allow the decay of almost all hadrons and allows to suppress line-of-sight particles The resulting muon beam then enters the Detector Solenoid and hits an aluminum stopping target: the muons can then be captured by the atoms and decay or convert into electrons, whose momentum and energy are measured by the cylindrical-shaped tracker and the two-disk calorimeter, respectively.

1.3 Signal and Predominant background

Mu2e experiment will search for process $\mu^- + N \rightarrow e^- + N$, where N is a nucleus of atomic mass A and atomic number Z. The conversion of a muon to an electron in the field of a nucleus is coherent: the muon recoils off the entire nucleus and the kinematics are those of two-body decay. Seen that the mass of a nucleus is large compared to the electron mass the recoil terms are small. A conversion electron is therefore monoenergetic with energy slightly less than the muon rest mass. The muon energy of 105.6 MeV is well above the maximum energy of the electron from muon decay at 52.8 MeV; hence, the vast majority of muon decays do not contribute to background.

When a negatively charged muon stops in a target it rapidly cascades down to the 1S state. Capture, decay or conversion of the muon takes place with a mean lifetime that has been measured in various materials and ranges from less than ~ 100 ns (high-Z nuclei) to over 2μs (low-Z nuclei). Depending of the target nucleus electron energy will be slightly less than the rest mass of the muon, as shown in 2

$$E_{\mu e} = m_{\mu}c^2 - E_b - \frac{E_{\mu}^2}{2m_N} \tag{2}$$

where m_{μ} is the muon mass, $E_b = Z^2\alpha^2 m_{\mu}/2$ is the atomic binding enrgy of the muon and last term is from nuclear recoil energy. For Al (Z = 13), a currently favored candidate nucleus, the conversion electron has energy $E_{\mu e} = 104.97$ MeV.

Mu2e goal is to reach sensitivity of $10^{-16} - 10^{-17}$ on $R_{\mu e}(Al)$ which is more than four order of magnitude beyond the current limit as shown in Fig 2

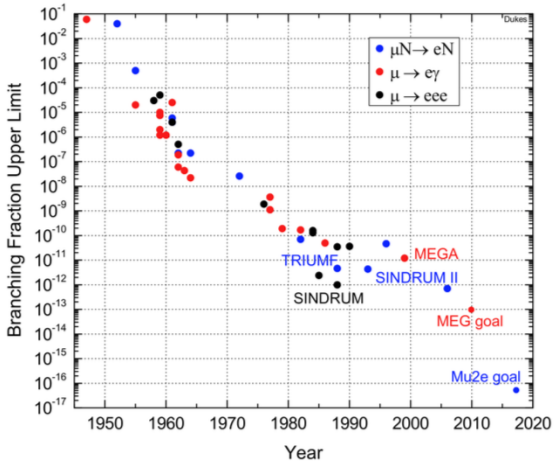

Figure 2: History of CLFV experiments

At this this value of sensitivity there are several processes that simulate the muon to electron conversion signal, such as:

- **muon decay-in- orbit (DIO)**: if the muon is bound in atomic orbit an electron produced in the decay can exchange momentum with the nucleus. A small probability to have an electron with a maximum possible energy equal to that of a conversion electron exists.
- **radiative muon capture (RMC)** $\mu^- Al \to \gamma\nu Mg$: intrinsic source of high energy photons that can convert to an

electron-positron pair in the stopping target or other surrounding material, producing an electron near the conversion electron energy. To reduce this background the stopping target is chosen so that the minimum masses of daughter nuclei are all at least a couple of MeV/c^2 above the rest mass of the stopping target nucleus, in order to push the RMC photon energy below the conversion electron energy.

- **presence of antiprotons**: they can be coincident in time with a conversion electron, simulating the energy of a conversion electron signal. The products of their interaction with the matter can be also a source of background.

- **radiative pion capture**: pions can produce background through the capture by the nucleus: $\pi^- + N \rightarrow \gamma N^*$

  because the kinetic endpoint has a peak at ~ 110MeV and also because producted photons convert in pairs. This kind of background can be reduced with an appropriate signal time window.

- **presence of cosmic rays(electrons, photons, muons)**: potential source of electrons near the conversion electron energy. If such electrons have trajectories that appear to originate in the stopping target they can fake a muon conversion.assive shielding and veto counters around the spectrometer and particle identification help to suppress this background electron

- **misreconstructed events**: to avoid this source of background it result fundamental to reduce high momentum resolution tails.

2 TRACKER GEOMETRY

[3] [4]

2.1 Tracker features

Mu2e tracker will measure electrons trajectory in order to calculate heir momentum. Tracker resolution plays an important role in determinig the level of background: errors in patern

recongnition can reduce acceptance of the signal and generate background. In Fig 3 is shown that the signal distribution has a peak not at the conversion energy, that is $p = 104.95 MeV/c$ (for Al) but around 104 MeV/c because of the energy loss. We expect for signal distribution a $\sigma \approx 350 keV/c$.

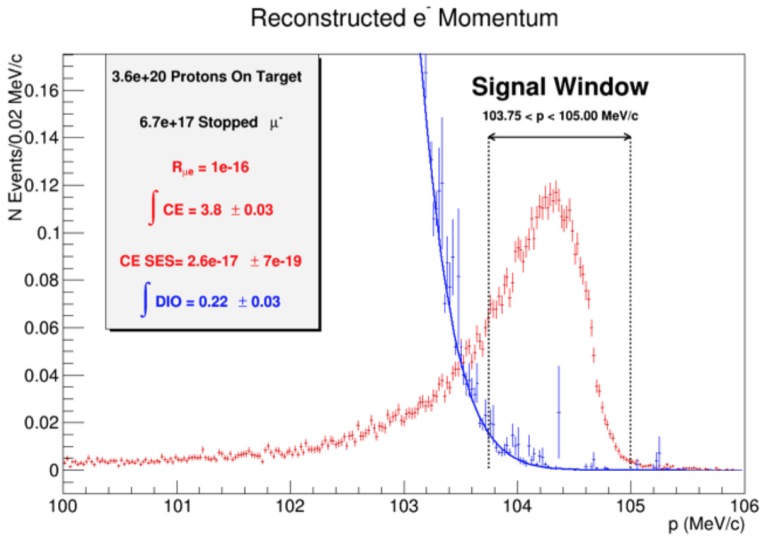

Figure 3: Reconstructed momentum spectrum for DIO (blue) and conversion electron(CE) events surviving selection criteria and normalized to the total number of muon stop for 3.6×10^{20} POT

Tracker resolution is an important component in determining the level of several critical backgrounds. The tracker is required to have a high-side resolution of $\sigma \sim 120$ - 180 keV, in this region tails fall steeply down, it results easy to misreconstruct a background event and consider it as signal. Misreconstruction can deal with mis-assignment of drift directions : even if drift radii are known it results impossible to measure drift directions as shown in Fig 4: the red straight line represents the electron trajectory within the tracker, blue lines represent multiple way to obtain a straight line tangent to the drift radii we calculated.

On the other hands requirement on the low-side tail is less stringent since background is smeared away from the signal region and it only causes acceptance loss of the signal.

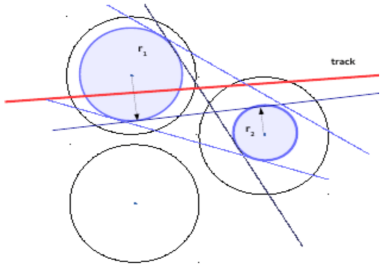

Figure 4: sketch mis-identification of drift direction

2.2 Current tracker geometry

The main aim of Mu2e tracker are:

- minimize multiple Coulumb scattering and enegy loss
- provide redundancy to protect against mis-reconstructions and non-Gaussian tails
- provide sufficient numbers of hits to find and fit tracks with high efficiency
- have segmentation and/or multi-hit capability to operate at the expected rates

Tracker total leght is ~3 m and the external diameter of each ring is 1.6 m, it is locate in a region with 1 T uniform magnetic field and its active area's radius extends from 40 to 70 cm, so that , as shown in Fig. 5 particles with a very low momentum enter directly in the central hole or the number of hits they product are not enough to reconstract a track in order to increase tracker purity.

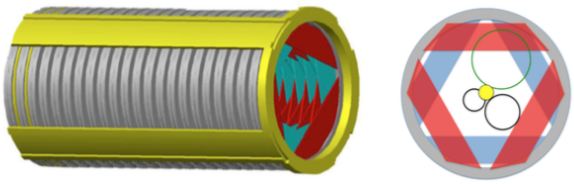

Figure 5: Cross view of Mu2e tracker with trajectories of a 105 MeV/c momentum conversion electron (top), 53 MeV/c Michel electron (bottom right) and electron with energy small than 53 MeV (bottom left)

The detector is made of 20736 **drift straw tubes** places transverse to the axis of the DS. Current choice for drift gas is 80:20

Argon: CO_2 with an operating voltage of$\leqslant$ 1500 V.

Straws features are presented in table 2

Sense wire	25µm
Tube diameter	5 mm
Thickness	15µm(Mylar)
Lenght	334÷ 1174
Gap between straws	1.5 mm

Table 2: Overview of straws parameters

As shown in Fig 6 groups of 96 straws are assembled into **panels**; in order to reduce the "righ-left ambiguity" each of them covers a 120° with two layers of straws. In other words these two layer of straws allows to determine easily on which side of the wire a track is passed.
Six panel are assembled into a **plane**. A face of a plane is made

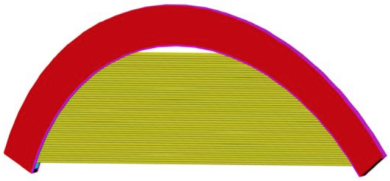

Figure 6: sketch of completed panel

of three panels, which are roteted by 30° as shown in Fig **??**.
A pair of planes made a **station**, each station is separated by 46 mm. This two planes are identical but the second plane is rotated 180 ° around ge vertical axis.

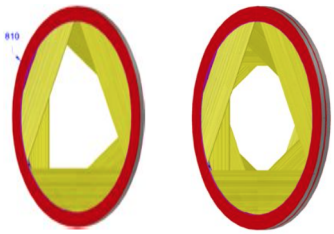

Figure 7: Left: Isometric view of tracker plane, it is possible to distinguish the two different faces made by three panels. Right: Station view, each station is made of two planes

2.3 Why thinking on tracker new configuration for Mu2e-2

Mu2e phase 2 will use PiP-II beam, it consist in a high energy linac which provides proton beam for Long Baseline Neutrino

facility. As shown in Fig 8 expected Mu2e-II background is three times higher than that expected for Mu2e and efficiency of the existing algorithm falls down by a factor of 2. Therefore Mu2e is looking for ways to make tracking more robust and increase performances.
A new configuration, based on making two faces on the same plane parallel, can improve track search decreasing momentum uncertainty due to the determination of drift directions. In this way hits in the same plane sit on a straght line

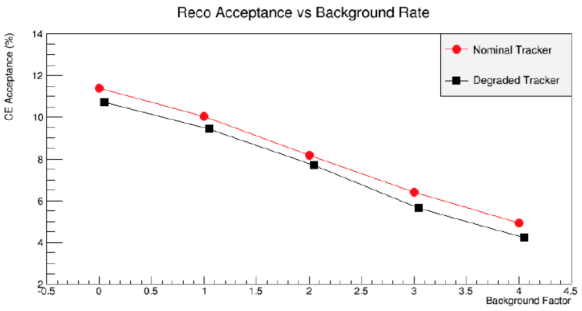

Figure 8: sketch of completed panel

As shown in fig 9 in current configuration knowing drift time is not enough to determine the drift direction: mis-identification of drift direction shifts the reconstructed track several mm away from the real one, affecting momentum reconstruction and consequently causing the increase of high-momentum tails of the resolution.

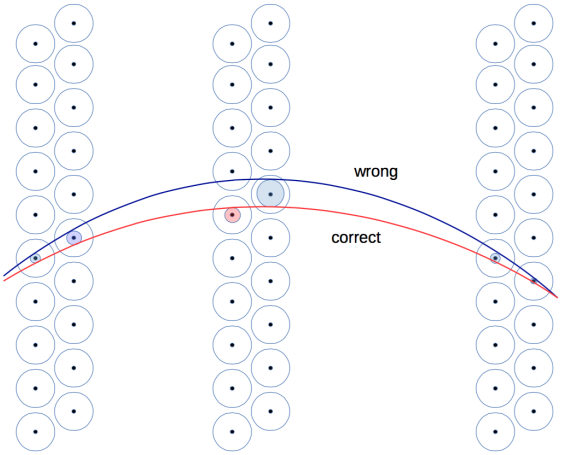

Figure 9: Origin of mis-reconstruction: the two track have similar dritf time in all straws except in one. At this point there is no way to determine the correct drift direction.

Let us consider a zoomed view of a reconstructed event; because of the rotation of the faces hits jump from one panel to another. It results difficult to identify a trajectory made by hits produced by the same particle.
If we consider configuration we descrideb above track reconstruction will be seed by 3-4 o more hit segment rather than by individual hits.

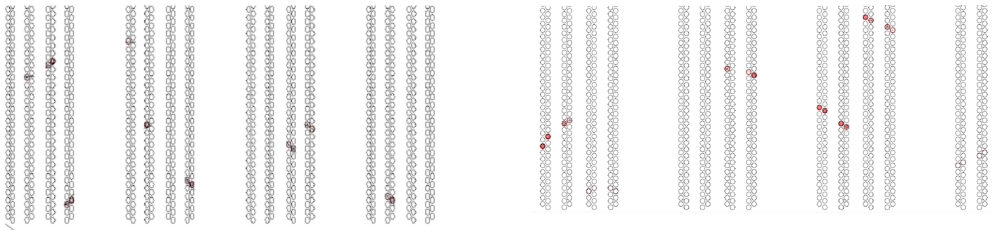

Figure 10: current (left) and proposed (right) tracker configuration side view

3 SEGMENT RECONSTRUCTION ALGORITHM AND PRELIMINARY RESULTS

The first step to study in this new configuration is to understand whether we can reconstruct enough segments to seed the track search.

Fig 11 represents the distribution of the number of plane with 3 or more hits. it results that the mean number of reconstructed segment allows us to reconstruct the track without efficiency loss in fact we fixed that segments should have at least three hits to be taken into account

Le us consider a plane as our build block, in order to define a segment in a plane we are intersted in reconstructing a straight line tangent to four circle.
We fix an hit in the first and the last straw layer, we determine slope and intercept of the straight line passing through this points using:

$$a = \frac{x_2 - x_1}{z_2 - z_1}, b = \frac{z_2 x_1 - z_1 x_2}{z_2 - z_1} \tag{3}$$

where a is the slope, b the intercept, z the plane coordinate along the beam line and x the straw coordinate. Then we run

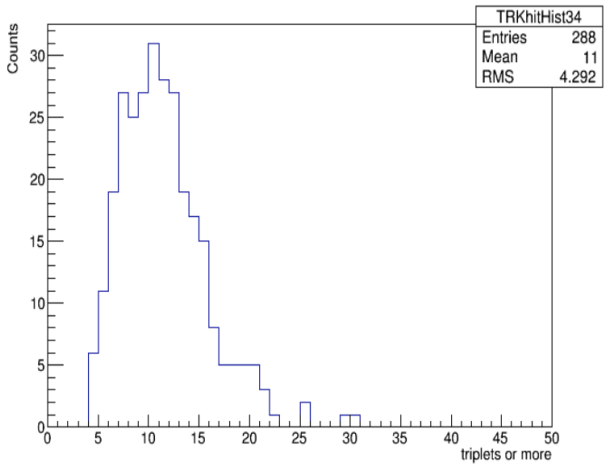

Figure 11: Number of planes with 3 or more hits

over all the other hits in the central straw and we calculate the distance between hits and segment as:

$$d = \frac{x_0 - az_0 - b}{\sqrt{1 + a^2}} \tag{4}$$

with (z_0, x_0) coordinates of a hit in the central layer.If distance is small compared to a $d_{max} = 10$ mm the hit is added to the list segment candidate. We fixed d_{max} arbitrarily so that we can consider four hits as segment candidate,(Fig 12) if their distance from the straight line is lower than the straw tube diameter.

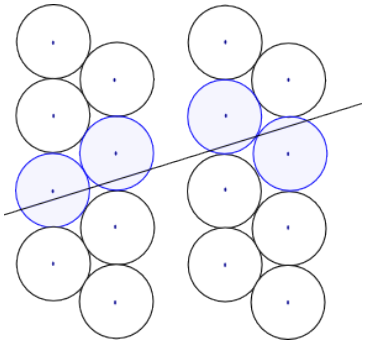

Figure 12: sketch of a segment candidate

At this point we want to evaluate segment candidate slope, intercept and time when a particle hit the straw we are considering.
We calculate residual $\Delta x_i = az_i + b - x_i - vt_{drift}$ in order to evaluate the χ^2,minimize it and find parameters we are interested in. It's important to underline that we cannot measure dritf

times directly but we know propagation time(t_{prop}) due to electronic and the measured time (t_i) so that $t_{drift} = t_i - t_prop - t_{0_i}$. Since distance between straw are small we can assume that all t_{0_i} are the same and calculate χ^2:

$$\chi^2 = \sum_i \Delta x_i^2 = \sum_i (az_i + b - x_i - vs_i (t_i - t_0))^2 \qquad (5)$$

where s_i is the drift direction.
It turns out that calculation of parameter is a linear problem, hence given a combination of drift signs it can be solved analitycally.
However we have to split the problem into cases:

- **Degenerate case**: all drift directions are the same
- **Non- Degenerate case**: drift direction are different

In the first situation it results impossible to determine separately b and t_0 but we can still calculate the slope and the residual if we fix $t_0 =< t >= \sum_i t_i/N$. In Figure 13 are sketched these two different cases. The number of segment candidates we obtain is equal to the number of all possible drift direction combination.

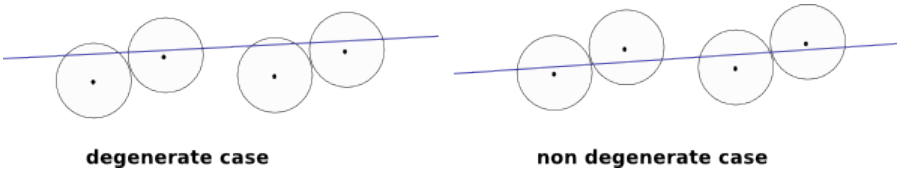

Figure 13: sketch of degenerate (left) and non-degerate(right) case

We fixed some conditions that a segment candidate has to verify to be consider as a track segment:

- $< t > \geqslant t_0$, that is the drift radius has to be positive
- $t_{drift_{max}} > \Delta t$ where $\Delta t =< t > -t_0$ and $t_{drift_{max}} = 50$ ns, we impose that the drift radius has to be less than the straw tube radius.
- the segment has to be the smallest χ^2 among all the possible combination
- the segment has to belong to an event that generates a track

To be sure that the way we are reconstructing drift direction is correct we define a parameter called seg_reco_flag which tells us how often our prediction corresponds to the Monte Carlo one.
If this parameter is equal to 0 dritft directions are misreconstructed, otherwise calculated and predicted drift direction are the same. As shown in Figure 14 our algorithm has to be improved because at this moment the number of events in which we reconstruct properly the drift direction is lower than the one in we mis-identify the drift direction.

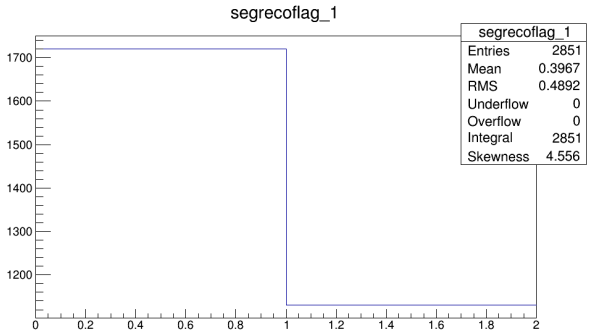

Figure 14: segrecoflag distribution.

One source of mis-identification of drift direction derives from segments made of hits with small drift time, in fact has we show in Figure 15 a flip in a drift direction does not affect the χ^2 value.

In Figure 16 is shown the best χ^2 distribution; we define best χ^2 the distribution made considering only segments which pass the selections we described previously. It results that χ^2 distribution is well consistent with the local coordinates of the tracker and uncertainty in segment reconstruction descrease: in current configuration uncertainty are comparable with the straw tube radius whereas with the proposal configuration we expected uncertainty of the order of several μm.

In Figure 17 is shown the segment slope distribution. For the majority of the entries we obtain

$$\left|\frac{dr}{dz}\right| < 2 \tag{6}$$

This range well approximate an helicoidal trajectory.

In Figure 18 jump to the particle track t_0,that is the time when a particle arrives in the middle of the track at z=0. We compare particle t_0 with the MC one. From the result of a gaussian fit we

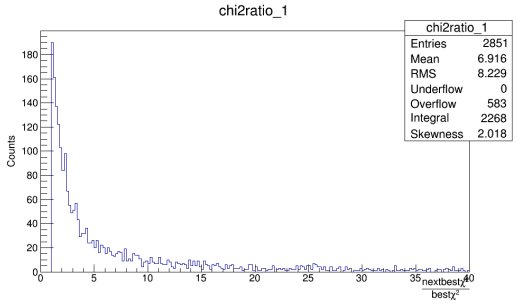

Figure 15: ratio between next best χ^2 and best χ^2

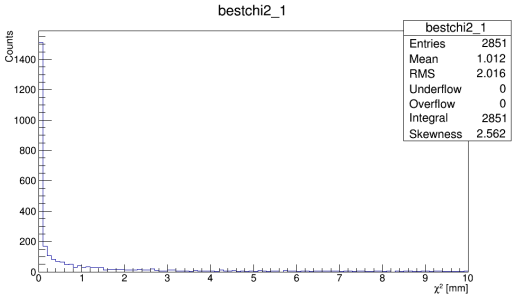

Figure 16: bestχ^2 distribution

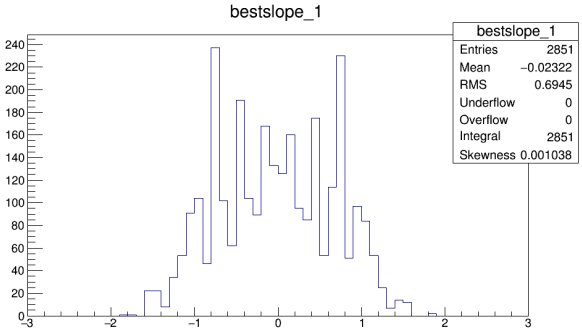

Figure 17: slope distribution

obtain $\sigma = (8.773 \pm 1.117)$ ns. This result is promising because it result smaller than the microbunch time and the $t_{drift_{max}}$

In conclusion we show that our algorithm does not involve a loss in efficiency, in fact we calculate the number of segment per track reconstructed and we see in Figure 19that the mean numer of segment is greater than two, minimum number of segment necessary to seed the track reconstruction.

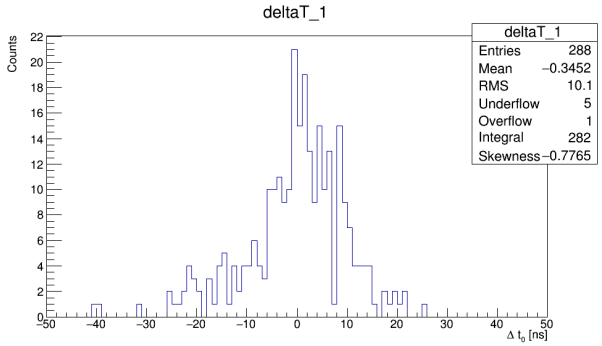

Figure 18: residual of $t_{0_{rec}}$ and $t_{0_{MC}}$ distribution

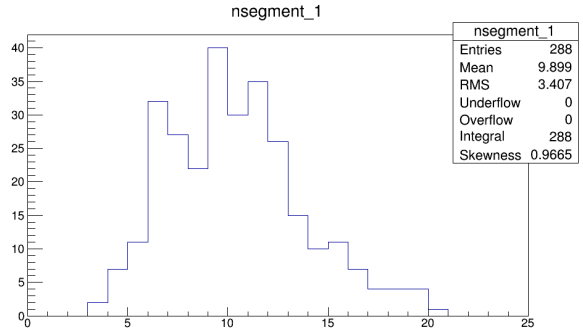

Figure 19: numeber of hits segment per track reconstructed distribution

4 CONCLUSION

This work presented represent just one of the first steps in for a new pattern recognition algorithm, which should improve track search performances at high background rate, in fact we maily focused in the segment finding rather that track reconstruction. However the results we obtain are promising, in fact they are in agreement with our assumption and expectation.
t is important to underline that what is presented is just a preliminary result. These first distributions are very important because they allows us to understand what kind of selection criteria should be applied in order to reject background. Moreover the possibility of knowing t_0 could make the first step of the track reconstruction more accurate.

REFERENCES

[1] Mu2e Collaboration. Mu2e Technical Design Report. *Fermi National Accelerator Laboratory*, 2014

[2] R. Bernstein, P.S. Cooper. Charged lepton flavor violation: An experimenter's guide. *Fermi National Accelerator Laboratory*, 2013

[3] R. Bernstein. Tracker Requirements Document. *Mu2eDocDB 732-v20*,2014

[4] P.Murat, G. Pezzullo. Mu2e Track Momentum Resolution: Understanding the High Side Tail. *Mu2eDocDB 5304-v7*,2015